Angewandte Chemie
Eine Zeitschrift der Gesellschaft Deutscher Chemiker

Supporting Information

Construction of Co–Mn Prussian Blue Analog Hollow Spheres for Efficient Aqueous Zn-ion Batteries

*Yinxiang Zeng, Xue Feng Lu, Song Lin Zhang, Deyan Luan, Sheng Li, and Xiong Wen (David) Lou**

anie_202107697_sm_miscellaneous_information.pdf

Experimental details

Synthesis of CoMn-glycerate solid spheres (SSs): CoMn-glycerate SSs were synthesized by a solvothermal reaction based on our previously reported works with slight modifications. In a typical synthesis, 75.3 mg of $Mn(NO_3)_2 \cdot 4H_2O$ and 21.8 mg of $Co(NO_3)_2 \cdot 6H_2O$ were dissolved into a mixture solution containing 8 mL of glycerol and 40 mL of isopropanol. After stirring for 20 min, the transparent solution was transferred into a Teflon-lined stainless steel autoclave. The solvothermal reaction was kept at 140 ^oC for 6 h. After cooling down to room temperature naturally, the precipitate was collected by centrifugation, washed with ethanol several times.

Synthesis of CoMn-PBA hollow spheres (HSs): Half of the as-prepared CoMn-glycerate SSs was dispersed into 100 mL of ethanol by sonication for 15 min to form solution A. 1.6 mmol of $K_4[Fe(CN)_6] \cdot 3H_2O$ was dissolved in 60 mL of deionized water to form solution B. Solution B was added into Solution A under stirring, and then heated in an oil bath at 90 ^oC for 4 h under reflux. The precipitate was collected by centrifugation, washed with water and ethanol several times. CoMn-PBA HSs with different Co to Mn atomic ratios were prepared with the same procedure, but with different amount of $Mn(NO_3)_2 \cdot 4H_2O$ and $Co(NO_3)_2 \cdot 6H_2O$ when preparing CoMn-glycerate SSs (70.6 mg of $Mn(NO_3)_2 \cdot 4H_2O$ and 27.3 mg of $Co(NO_3)_2 \cdot 6H_2O$ for CoMn-PBA-1-3 HSs, and 78.4 mg of $Mn(NO_3)_2 \cdot 4H_2O$ and 18.2 mg of $Co(NO_3)_2 \cdot 6H_2O$ for CoMn-PBA-1-5 HSs).

Synthesis of Mn-glycerate and Co-glycerate SSs: The synthesis methods for Mn-glycerate and Co-glycerate SSs are similar to that of the CoMn-glycerate SSs. 94.1 mg of $Mn(NO_3)_2 \cdot 4H_2O$ or 109.1 mg of $Co(NO_3)_2 \cdot 6H_2O$ was dissolved into a mixture solution containing 8 mL of glycerol and 40 mL of isopropanol. After stirring for 20 min, the transparent solution was transferred into a Teflon-lined stainless steel autoclave. The solvothermal reaction was kept at 180 ^oC for 6 h. After cooling down to room temperature naturally, the precipitate was collected by centrifugation, washed with ethanol several times.

Synthesis of Mn-PBA HSs: Half of the as-prepared Mn-glycerate SSs was dispersed into 100 mL of ethanol by sonication for 15 min to form solution A. 2.4 mmol of $K_4[Fe(CN)_6] \cdot 3H_2O$ was dissolved in 60 mL of deionized water to form solution B. Solution B was added into Solution A under stirring, and then heated in an oil bath at 90 ^oC for 5 h under reflux. The precipitate was collected by centrifugation, washed with water and ethanol several times.

Synthesis of Co-PBA HSs: Half of the as-prepared Co-glycerate SSs was dispersed into 80 mL of isopropanol by sonication for 15 min, and then 5.6 g polyvinylpyrrolidone (M_w = 58000) was added under stirring to form solution A. 2.4 mmol of $K_4[Fe(CN)_6]\cdot 3H_2O$ and 2.8 mmol of trisodium citrate dihydrate were dissolved in 80 mL of deionized water to form solution B. Solution B was added into solution A under stirring, and then heated in an oil bath at 100 ^oC for 3 h under reflux. The precipitate was collected by centrifugation, washed with water and ethanol several times.

Synthesis of CoMn-PBA nanocubes (NCs): CoMn-PBA NCs were prepared by a co-precipitation method. 0.12 mmol of $Co(Ac)_2\cdot 4H_2O$, 0.48 mmol of $Mn(Ac)_2\cdot 4H_2O$, and 0.5 mmol of trisodium citrate dihydrate were dissolved in 40 mL of deionized water to form solution A. 0.4 mmol of $K_3[Fe(CN)_6]$ was dissolved in 60 mL of deionized water to form solution B. Then, solution B was added into solution A under magnetic stirring in 15 s. After stirring for 1 min, the obtained solution was aged for 24 h at room temperature. The precipitate was collected by centrifugation, washed with water and ethanol several times.

Synthesis of CoMn-PBA-350 HSs: Half of the as-prepared CoMn-glycerate SSs was dispersed into 120 mL of isopropyl alcohol by sonication for 15 min to form solution A. 1.6 mmol of $K_4[Fe(CN)_6]\cdot 3H_2O$ was dissolved in 40 mL of deionized water to form solution B. Solution B was added into Solution A under stirring, and then heated in an oil bath at 80 ^oC for 4 h under reflux. The precipitate was collected by centrifugation, washed with water and ethanol several times.

Material characterizations: The morphology and structure of the samples were characterized by field-emission scanning electron microscope (FESEM; JEOL-6700F) and transmission electron microscope (TEM; JEOL, JEM-2010). Elemental mapping images were collected using a TEM (JEOL, JEM-2100F) equipped with energy dispersive X-ray (EDX) spectroscopy. The composition was analyzed by EDX spectroscopy attached to the FESEM instrument. The crystal phases of the samples were analyzed by X-ray diffraction (XRD) on a Bruker D2 Phaser X-Ray Diffractometer with Ni filtered Cu $K\alpha$ radiation (λ = 1.5406 Å) at a voltage of 30 kV and a current of 10 mA. The chemical states of the elements on the surface of the samples were evaluated by X-ray photoelectron spectrometer (XPS; ESCALAB 250). Fourier-transform infrared (FTIR) spectra were recorded by PerkinElmer FTIR spectrometers using the KBr pellet method. The specific surface area of the samples was calculated from the nitrogen adsorption isotherms measured with a Micrometrics ASAP 2010 based on the Brunauer-Emmett-Teller (BET) model. The samples were degassed in vacuum at 453 K for 15 h before analysis. Thermogravimetric

analysis (TGA) was performed on a SDT Q600 (TA Instruments) analyzer at a heating rate of 5 ^{o}C min^{-1} from 25 to 500 ^{o}C in N_2 atmosphere.

Electrochemical measurements. The working electrodes were prepared by pasting the slurry containing 70 wt% of active material, 20 wt% of ketjen black and 10 wt% of poly(vinyl difluoride) (PVDF) binder onto a carbon fiber paper. After that, the coated carbon fiber paper was dried in a vacuum oven at 80 ^{o}C for 12 h. The loading mass of active material is about 0.8-1.0 mg cm^{-2}. The electrolyte was 2.0 mol L^{-1} $Zn(CF_3SO_3)_2$ aqueous solution. A zinc foil with a thickness of 0.05 mm was used as the anode. Electrochemical characterization was carried out using 2032 type coin cells at room temperature. The galvanostatic discharge-charge tests were conducted on a Neware battery testing system (Neware, China) with a cut-off voltage range of 0.5-1.8 V versus Zn/Zn^{2+}. Cyclic voltammetry measurements were carried out on a CHI 760E electrochemical workstation (ChenHua Instruments Co., China). Galvanostatic intermittence titration technique (GITT) was conducted by a series of galvanostatic discharge pulses of 120 s at 50 mA g^{-1}, followed by a 1 h rest.

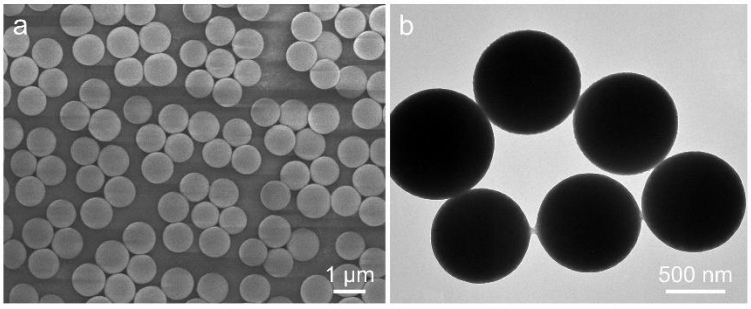

Figure S1. (a) FESEM and (b) TEM images of CoMn-glycerate SSs.

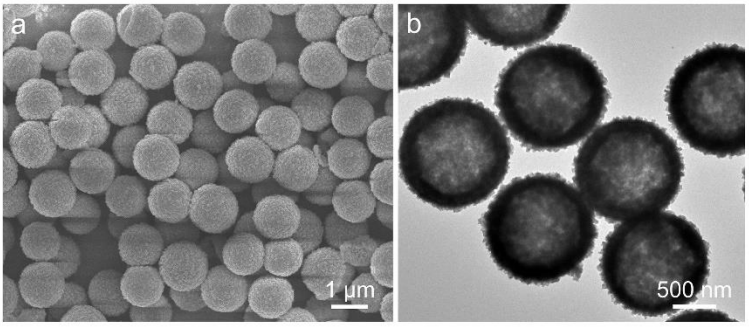

Figure S2. (a) FESEM and (b) TEM images of CoMn-PBA HSs.

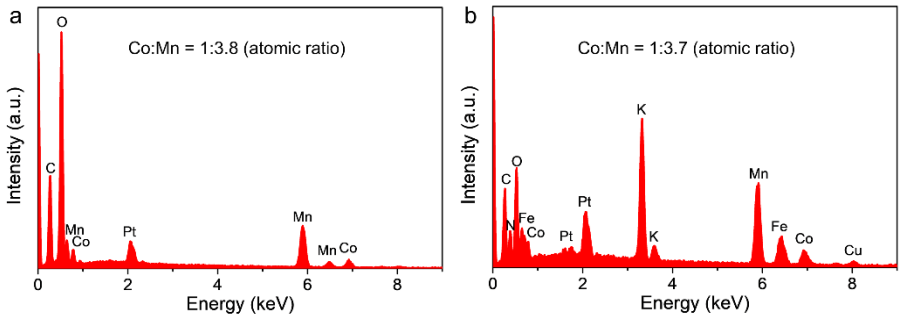

Figure S3. EDX spectra of (a) CoMn-glycerate SSs and (b) CoMn-PBA HSs.

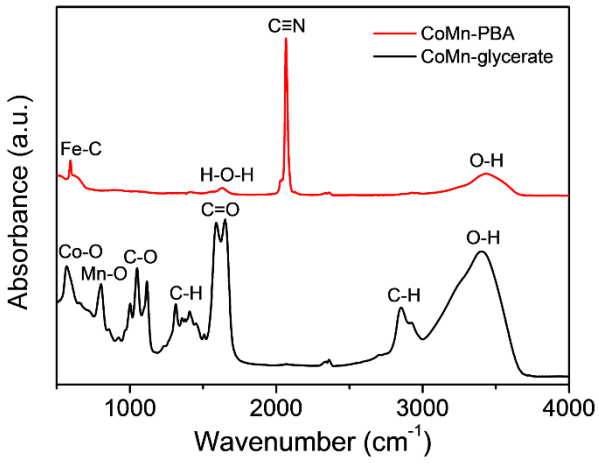

Figure S4. FTIR spectra of CoMn-glycerate SSs and CoMn-PBA HSs.

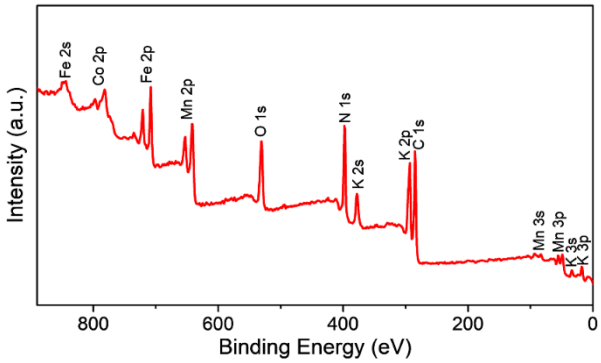

Figure S5. XPS survey spectrum of CoMn-PBA HSs.

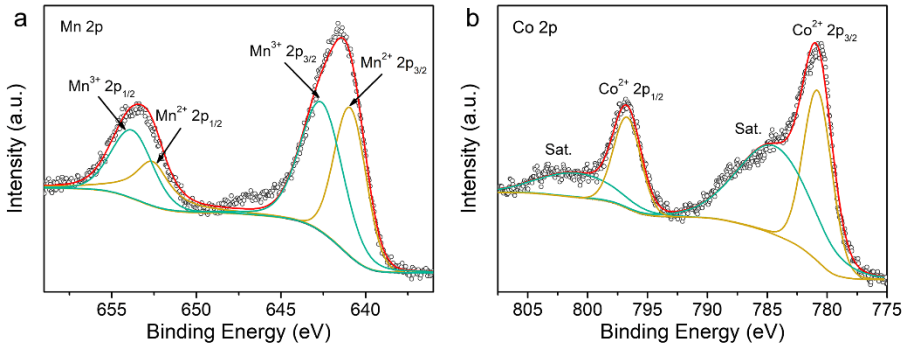

Figure S6. High-resolution XPS spectra of (a) Mn 2p for Mn-PBA HSs, and (b) Co 2p for Co-PBA HSs.

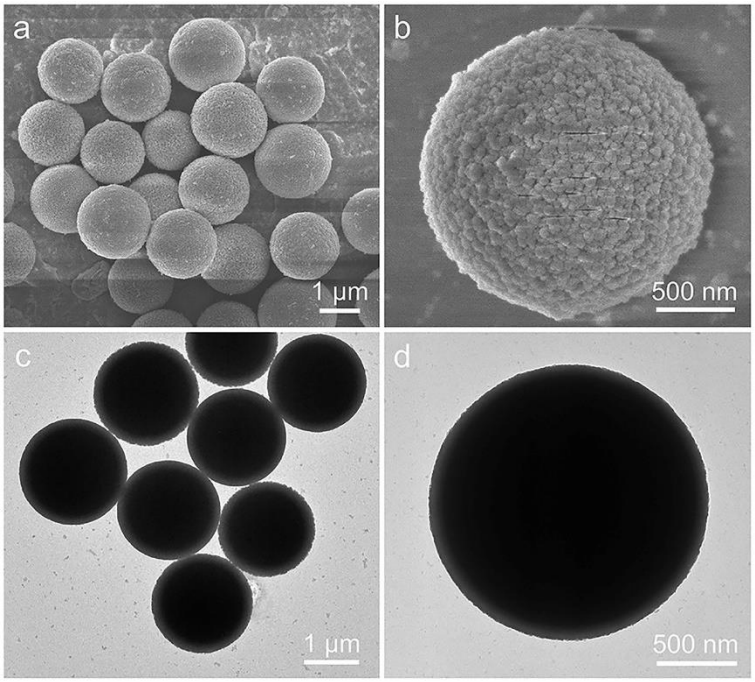

Figure S7. (a,b) FESEM and (c,d) TEM images of Mn-glycerate SSs.

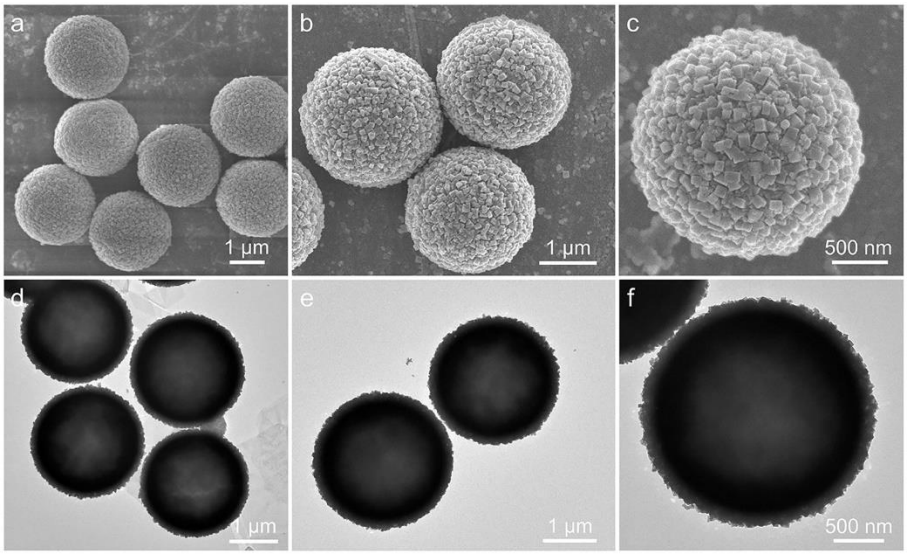

Figure S8. (a-c) FESEM and (d-f) TEM images of Mn-PBA HSs.

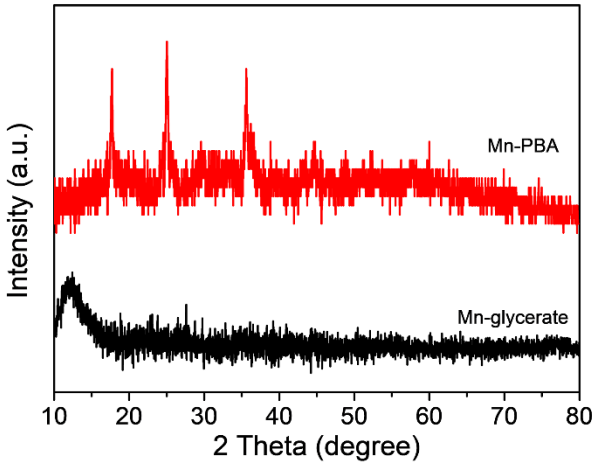

Figure S9. XRD patterns of Mn-glycerate SSs and Mn-PBA HSs.

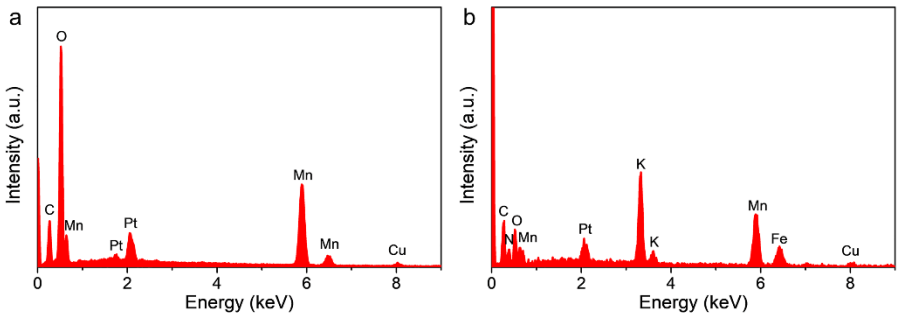

Figure S10. EDX spectra of (a) Mn-glycerate SSs and (b) Mn-PBA HSs.

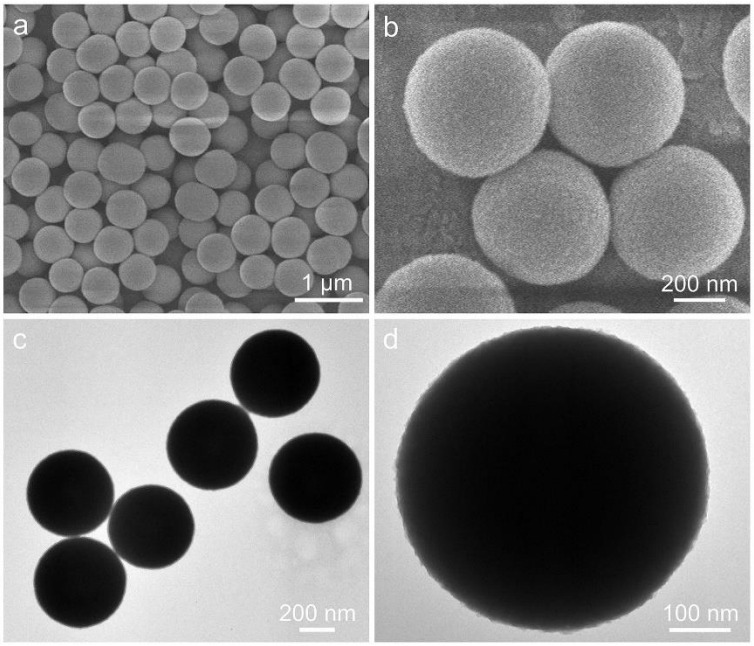

Figure S11. (a,b) FESEM and (c,d) TEM images of Co-glycerate SSs.

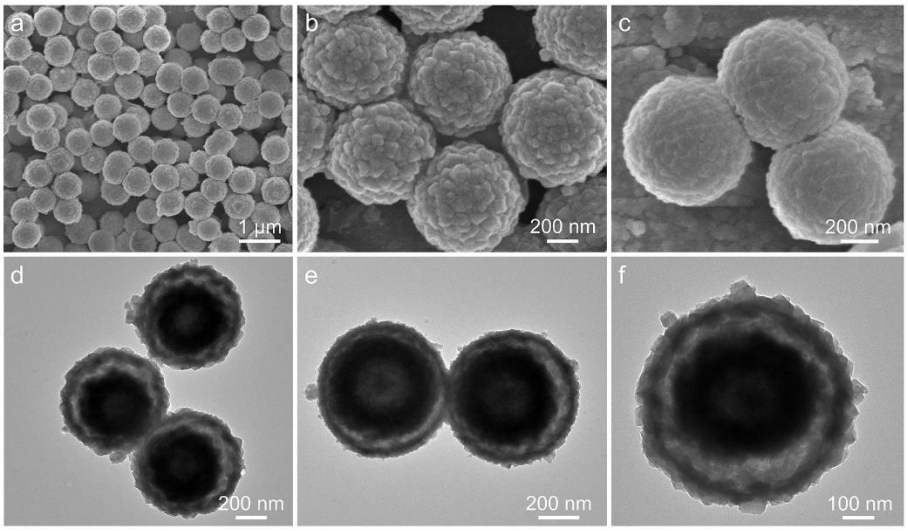

Figure S12. (a-c) FESEM and (d-f) TEM images of Co-PBA HSs.

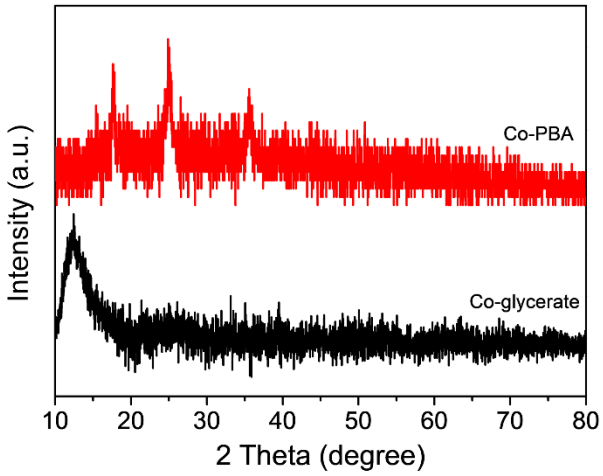

Figure S13. XRD patterns of Co-glycerate SSs and Co-PBA HSs.

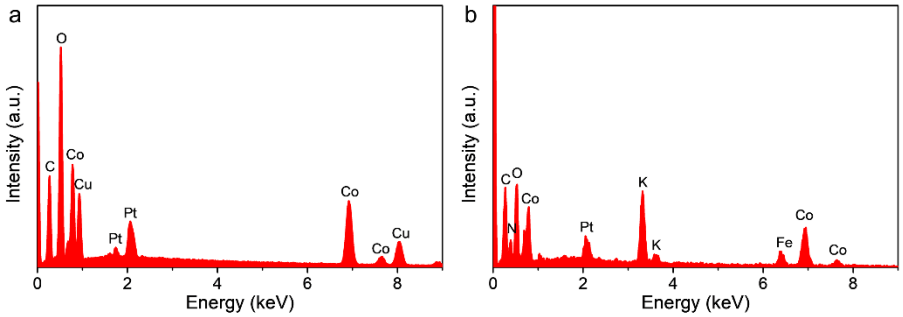

Figure S14. EDX spectra of (a) Co-glycerate SSs and (b) Co-PBA HSs.

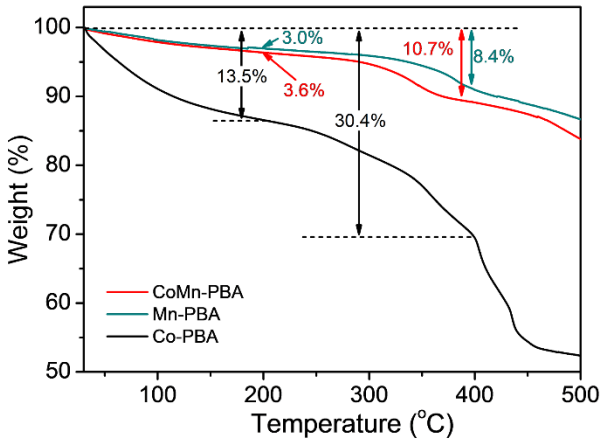

Figure S15. TGA curves of CoMn-PBA HSs, Mn-PBA HSs, and Co-PBA HSs tested under N_2 atmosphere. The weight loss below 200 °C generally originates from the loss of physically adsorbed water. And the weight loss between 200 and 400 °C steps from the loss of coordinated water.[1,2]

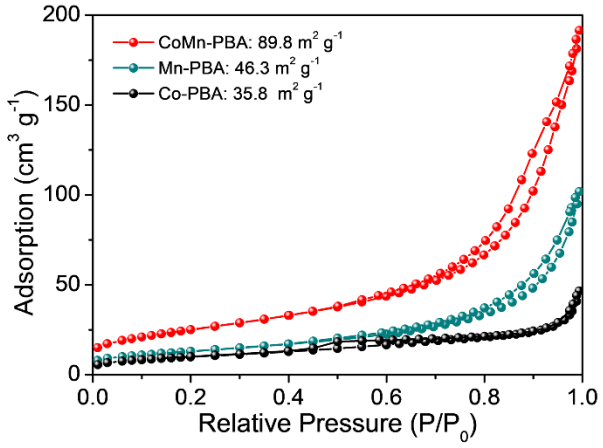

Figure S16. Nitrogen adsorption-desorption isotherms of CoMn-PBA HSs, Mn-PBA HSs, and Co-PBA HSs.

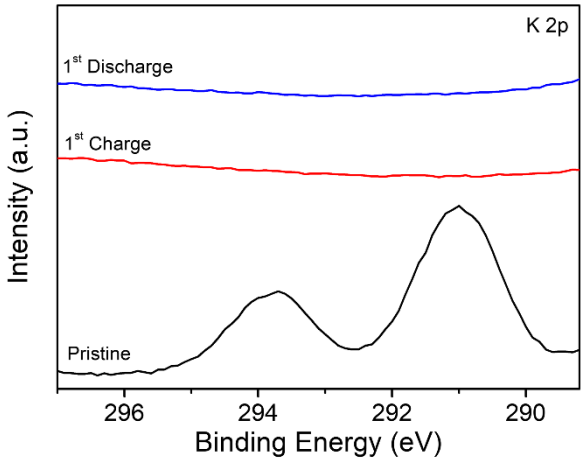

Figure S17. High-resolution K 2p XPS spectra of the pristine, first charged, and first discharged CoMn-PBA HSs.

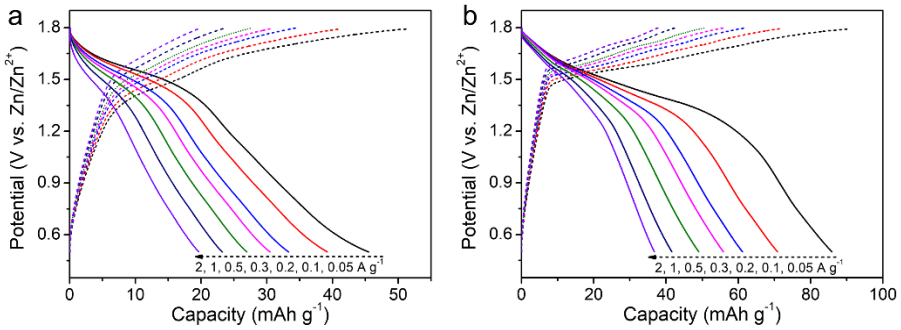

Figure S18. Charge-discharge voltage profiles of (a) Co-PBA HSs and (b) Mn-PBA HSs at various current densities.

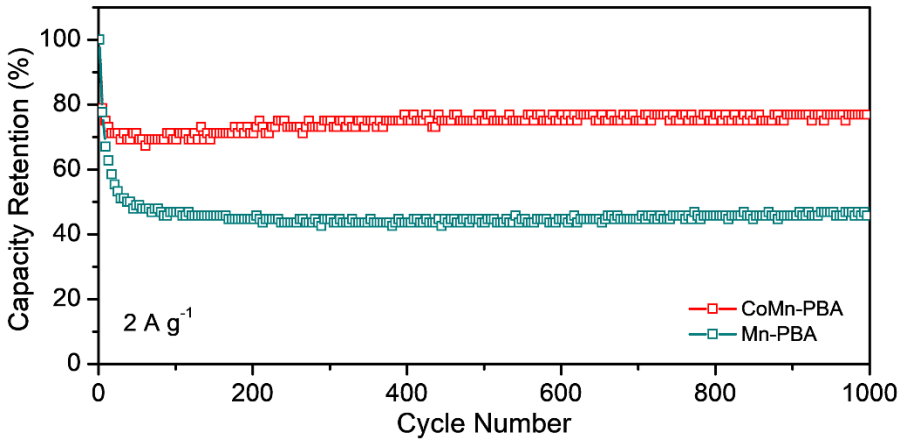

Figure S19. Cycling performance of CoMn-PBA HSs and Mn-PBA HSs tested at a current density of 2 A g^{-1}.

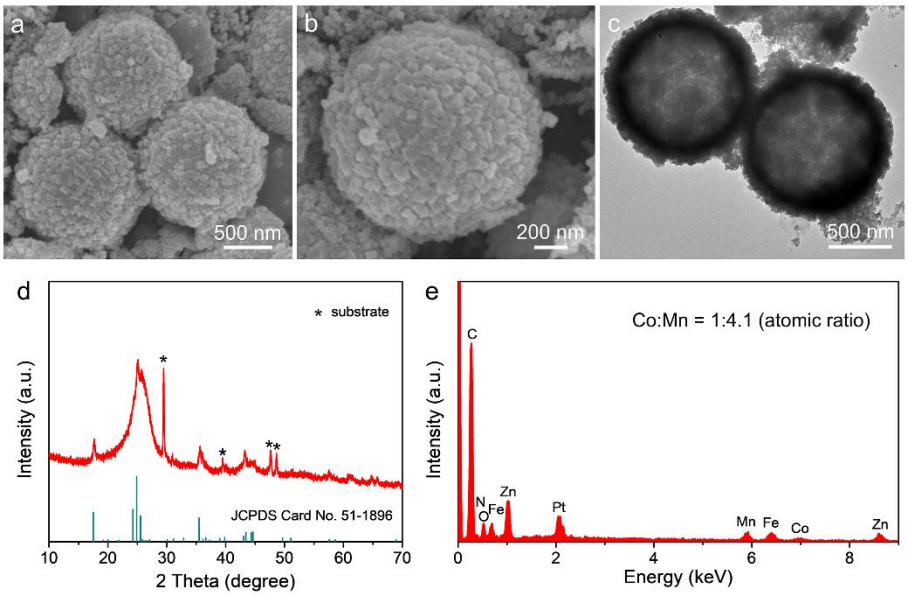

Figure S20. (a,b) FESEM images, (c) TEM image, (d) XRD pattern, (e) EDX spectrum of CoMn-PBA HSs after 1000 cycles at 1 A g^{-1}. The CoMn-PBA HSs still retains the spherical morphology with well-defined hollow structure. XRD and EDX results also confirm that the crystalline phase and composition of CoMn-PBA HSs are well preserved after 1000 cycles.

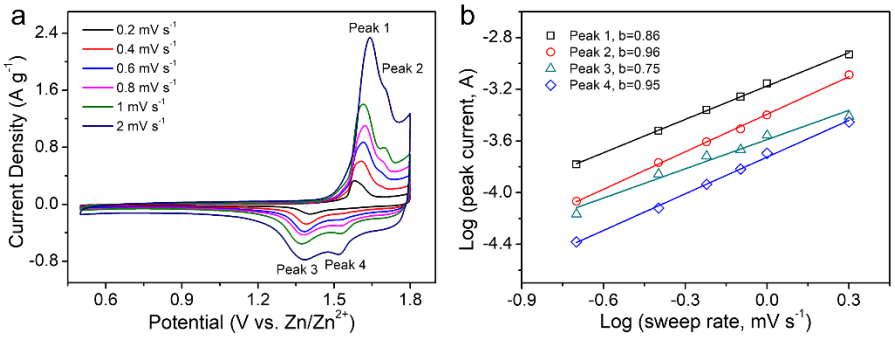

Figure S21. (a) CV curves of CoMn-PBA HSs at various scan rates. (b) Determination of the *b* value using the relationship between peak current and scan rate.

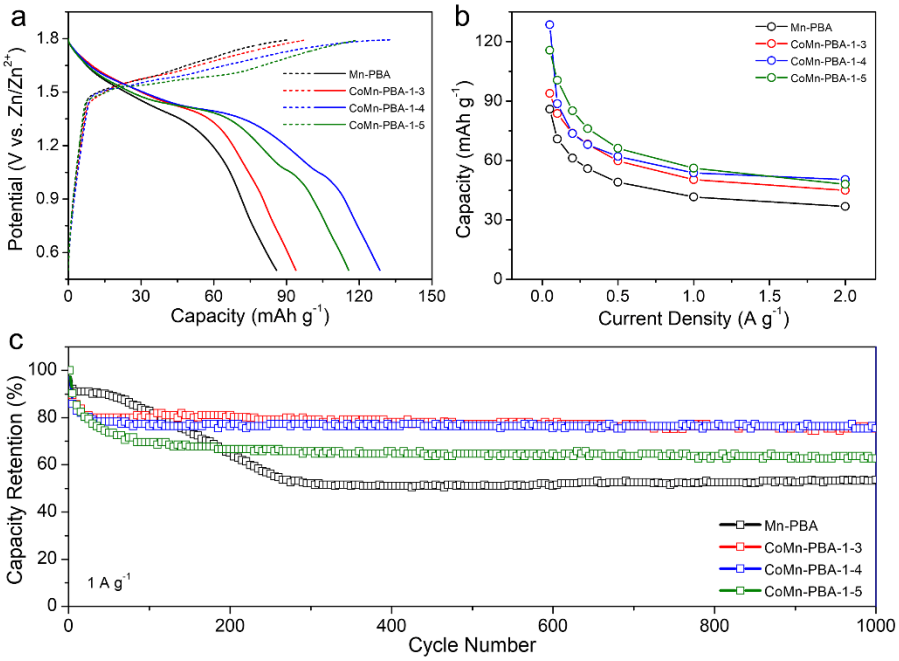

Figure S22. (a) Charge-discharge voltage profiles at a current density of 0.05 A g^{-1}, (b) discharge capacities at various current densities, (c) cycling performance tested at 1 A g^{-1} for the Mn-PBA HSs and CoMn-PBA HSs with different Co/Mn atomic ratios. CoMn-PBA HSs with different Co/Mn atomic ratios of 1:3, 1:4, 1:5 are denoted as CoMn-PBA-1-3, CoMn-PBA-1-4, CoMn-PBA-1-5, respectively.

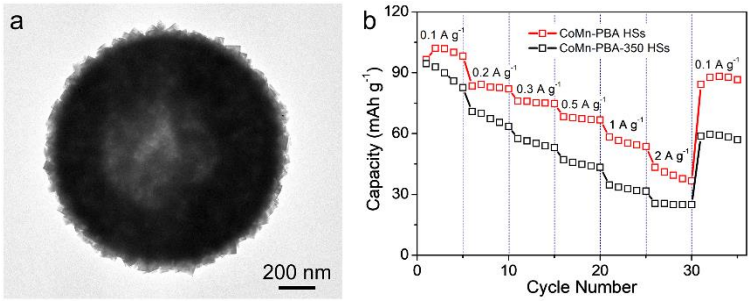

Figure S23. (a) TEM image of CoMn-PBA-350 HSs. (b) Rate performance based on discharge curves of CoMn-PBA HSs and CoMn-PBA-350 HSs. CoMn-PBA HSs with a shell of about 350 nm are denoted as CoMn-PBA-350 HSs. Compared with CoMn-PBA-350 HSs, the CoMn-PBA HSs electrode with thin shell shows higher capacity and better rate capability.

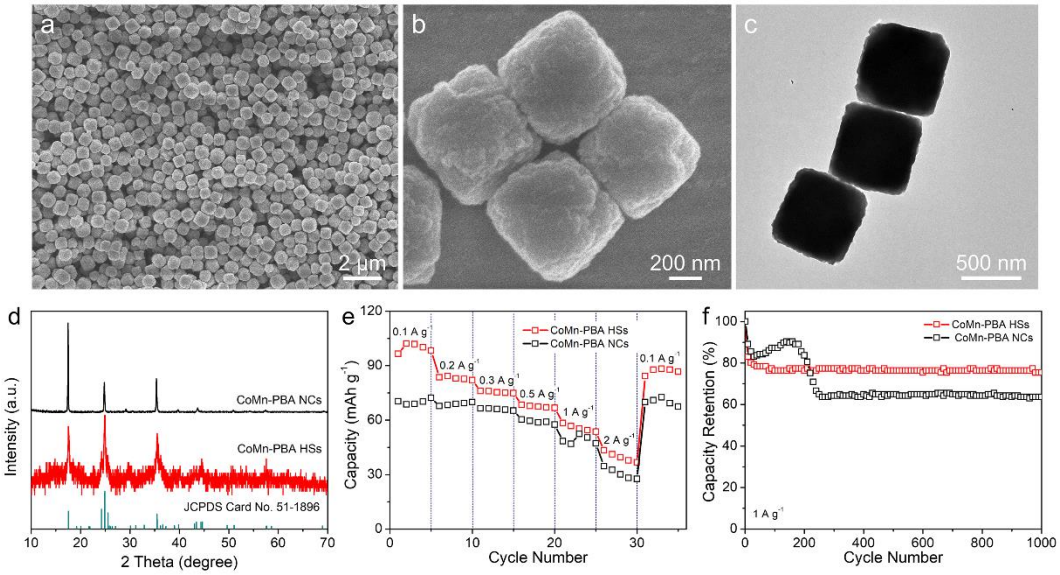

Figure S24. (a,b) FESEM and (c) TEM images of CoMn-PBA NCs. (d) XRD patterns, (e) rate performance based on discharge curves, (f) cycling performance tested at 1 A g^{-1} of CoMn-PBA HSs and CoMn-PBA NCs. FESEM and TEM images validate the nanocubic morphology and solid nature. XRD patterns of CoMn-PBA NCs and CoMn-PBA HSs are almost the same and both can be indexed well to $KMnFe(CN)_6 \cdot nH_2O$ (JCPDS card No. 51-1896). Electrochemical test results show that the CoMn-PBA HSs electrode exhibits higher capacity, better rate, and cycling performance than the CoMn-PBA NCs electrode, indicating that the CoMn-PBA HSs electrode with hollow structure can afford better zinc ion storage performance.

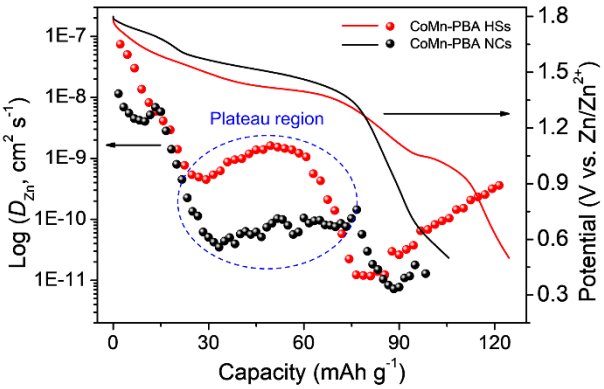

Figure S25. The D_{Zn} of CoMn-PBA HSs and CoMn-PBA NCs at discharge state tested at 0.05 A g^{-1} and corresponding discharge curves. The Zn^{2+} ions diffusion coefficient (D_{Zn}) of CoMn-PBA HSs at the discharge plateau region is obviously higher than that of CoMn-PBA NCs, suggesting that CoMn-PBA HSs allow faster Zn^{2+} ion diffusion.

Table S1. Comparison of electrochemical performance of PBA-based materials for aqueous rechargeable batteries.

Electrodes	Inserted ions	Capacity (mAh g^{-1}@A g^{-1})	Rate capability (mAh g^{-1}@A g^{-1})	Cycling performance	Ref.
CoMn-PBA	Zn^{2+}	128.6@0.05	50.4@2	75.4% (1000 cycles)	This work
CoMn-PBA	Na^{+}	112.8@0.06	-	80% (100 cycles)	[3]
Mn-PBA	Zn^{2+}	65@0.05	45@0.2	49% (200 cycles)	[4]
Fe-PBA	Zn^{2+}	76@1	41@8	82% (5000 cycles)	[5]
Zn-PBA	Zn^{2+}	65@0.065	-	70% (1000 cycles)	[6]
Zn-PBA	Zn^{2+}	65.4@0.06	32.3@1.2	76% (100 cycles)	[7]
Cu-PBA	Zn^{2+}	60@0.06	~36@3	83% (500 cycles)	[8]
Mn-PBA	Al^{3+}	106.3@0.2	54@1	69.5% (100 cycles)	[9]
Ni-PBA	NH_4^{+}	60@0.15	22@1.8	74% (2000 cycles)	[10]
Fe-PBA	K^{+}+Na^{+}	125@0.075	41@9	-	[1]
Fe-PBA	K^{+}	111@0.5	93@3	81% (500 cycles)	[11]
VFe-PBA	Na^{+}+H^{+}	94.1@0.055	54@3.52	61% (250 cycles)	[12]
Zn-PBA	Zn^{2+}+K^{+}	69.1@0.172	46.7@5.16	74.1% (500 cycles)	[13]
Co-PBA	Zn^{2+}+Na^{+}	~80@0.1	~45.6@5	~44% (400 cycles)	[14]
Cu-PBA	Zn^{2+}+NH_4^{+}	70.4@0.3	51.2@1.8	76.5% (1000 cycles)	[15]
Co-PBA	Al^{3+}	50@0.1	~18@1	71% (1600 cycles)	[16]
Co-PBA	Na^{+}	97.8@0.5	41.1@20	94% (5000 cycles)	[17]
NiCo-PBA	Na^{+}	85@0.035	44@0.7	90% (100 cycles)	[18]

Supplementary references:

[1] C. Liu, X. Wang, W. Deng, C. Li, J. Chen, M. Xue, R. Li, F. Pan, *Angew. Chem. Int. Ed.* **2018**, *57*, 7046.

[2] J. Li, L. He, J. Jiang, Z. Xu, M. Liu, X. Liu, H. Tong, Z. Liu, D. Qian, *Electrochim. Acta* **2020**, *353*, 136579.

[3] M. A. Oliver-Tolentino, J. Vázquez-Samperio, S. N. Arellano-Ahumada, A. Guzmán-Vargas, D. Ramírez-Rosales, J. A. Wang, E. Reguera, *J. Phys. Chem. C* **2018**, *122*, 20602.

[4] Q. Li, K. Ma, G. Yang, C. Wang, *Energy Storage Mater.* **2020**, *29*, 246.

[5] Q. Yang, F. Mo, Z. Liu, L. Ma, X. Li, D. Fang, S. Chen, S. Zhang, C. Zhi, *Adv. Mater.* **2019**, *31*, 1901521.

[6] X. Wu, Y. Xu, C. Zhang, D. P. Leonard, A. Markir, J. Lu, X. Ji, *J. Am. Chem. Soc.* **2019**, *141*, 6338.

[7] L. Zhang, L. Chen, X. Zhou, Z. Liu, *Adv. Energy Mater.* **2015**, *5*, 1400930.

[8] T. Gupta, A. Kim, S. Phadke, S. Biswas, T. Luong, B. J. Hertzberg, M. Chamoun, K. Evans-Lutterodt, D. A. Steingart, *J. Power Sources* **2016**, *305*, 22.

[9] D. Wang, H. Lv, T. Hussain, Q. Yang, G. Liang, Y. Zhao, L. Ma, Q. Li, H. Li, B. Dong, T. Kaewmaraya, C. Zhi, *Nano Energy* **2021**, *84*, 105945.

[10] X. Wu, Y. Qi, J. J. Hong, Z. Li, A. S. Hernandez, X. Ji, *Angew. Chem. Int. Ed.* **2017**, *56*, 13026.

[11] D. Su, A. McDonagh, S. Z. Qiao, G. Wang, *Adv. Mater.* **2017**, *29*, 1604007.

[12] J. H. Lee, G. Ali, D. H. Kim, K. Y. Chung, *Adv. Energy Mater.* **2017**, *7*, 1601491.

[13] M. Huang, J. Meng, Z. Huang, X. Wang, L. Mai, *J. Mater. Chem. A* **2020**, *8*, 6631.

[14] D. Zhang, Z. Yang, J. Zhang, H. Mao, J. Yang, Y. Qian, *J. Power Sources* **2018**, *399*, 1.

[15] C. Li, J. Wu, F. Ma, Y. Chen, L. Fu, Y. Zhu, Y. Zhang, P. Wang, Y. Wu, W. Huang, *ACS Appl. Energy Mater.* **2019**, *2*, 6984.

[16] Y. Ru, S. Zheng, H. Xue, H. Pang, *Chem. Eng. J.* **2020**, *382*, 122853.

[17] L. Ren, J. G. Wang, H. Liu, M. Shao, B. Wei, *Electrochim. Acta* **2019**, *321*, 134671.

[18] W. Li, F. Zhang, X. Xiang, X. Zhang, *J. Phys. Chem. C* **2017**, *121*, 27805.